First-principles study of metallic carbon nanotubes with boron/nitrogen co-doping*

Chen Ling-Na(陈灵娜)[a)b)], Ma Song-Shan(马松山)[a)], OuYang Fang-Ping(欧阳芳平)[a)], Xiao Jin(肖 金)[a)], and Xu Hui(徐 慧)[a)†]

[a)] *School of Physics Science and Technology, Central South University, Changsha* 410083, *China*
[b)] *School of Computer Science and Technology, University of South China, Hengyang* 421001, *China*

(Received 4 November 2009; revised manuscript received 17 January 2010)

Using the first-principles calculations, we investigate the electronic band structure and the quantum transport properties of metallic carbon nanotubes (MCNTs) with B/N pair co-doping. The results about formation energy show that the B/N pair co-doping configuration is a most stable structure. We find that the electronic structure and the transport properties are very sensitive to the doping concentration of the B/N pairs in MCNTs, where the energy gaps increase with doping concentration increasing both along the tube axis and around the tube, because the mirror symmetry of MCNT is broken by doping B/N pairs. In addition, we discuss conductance dips of the transmission spectrum of doped MCNTs. These unconventional doping effects could be used to design novel nanoelectronic devices.

Keywords: metallic carbon nanotube, B/N pairs co-doping, energy gap, first-principles
PACS: 71.15Mb, 71.55.–i, 73.22.–f **DOI:** 10.1088/1674-1056/20/1/017103

1. Introduction

Since 1991, carbon nanotubes (CNTs)[1] have attracted intensive research interest because of their unique physical properties[2−6] and future applications of nanoelectronic devices, such as field-effect transistors (FETs),[7,8] field emission sources,[9] chemical sensors,[10] memory[11] and hybrid devices.[12] However, the fabrication of these electronic devices with CNTs is difficult due to the mixture of both metallic and semiconducting CNTs. Recently, much effort has been made to selectively remove metallic CNTs from CNT devices composed of different types of CNTs. As is well known, doping is very useful for controlling the electronic band structure of carbon nanotubes. With the development of synthesis techniques, various kinds of doped CNTs have been fabricated.[13−17] Nitrogen and boron atoms have almost the same radii as the radius of carbon atom, and can be easily incorporated into carbon network, therefore they are naturally chosen as dopant. It is shown that either B or N atom alone is difficult to dope into metallic carbon nanotubes (MCNTs) lattices, while B and N atoms are more likely to co-dope into MCNTs by substituting a pair of B and N atoms for a pair of carbon atoms.[18] At present, boron and nitrogen atom pair co-doping CNTs have been synthesised by directly using chemical vapour deposition.[19]

Doped MCNTs have been theoretically investigated,[20,21] and the results show that pristine MCNT retains zero gap and doping by either B or N atom alone tends to produce metallic behaviour. Very recently, band gap engineering of B/N atom pair co-doping CNTs was experimentally demonstrated,[18] showing that MCNTs were successfully converted into semiconductors by B/N pair co-doping. To understand such phenomena observed in these experiments, we investigate the effect of B/N pair co-doping theoretically.

In this paper, we present an *ab initio* study of electronic structures and quantum transport properties of doped armchair MCNTs with B/N pairs. Here we study the influence of doping site on the formation energy of MCNTs. We also show how B/N pair co-doping affects the band structure of MCNTs. In particular, we calculate their transmission spectrum by using model metallic electrodes. Resonant energy modifies the conductance spectrum of the MCNTs by breaking the mirror symmetry. Our results may present a new way to modulate band structure of MC-

*Project supported by the National Natural Science Foundation of China (Grant Nos. 10325415 and 50504017), the Natural Science Foundation of Hunan Province, China (Grant No. 07JJ3102), the Scientific Research Fund of Hunan Provincial Education Department, China (Grant No. 10C1171), and the Science Development Foundation of Central South University, China (Grant Nos. 08SDF02 and 09SDF09).
†Corresponding author. E-mail: cmpxhg@mail.csu.edu.cn
© 2011 Chinese Physical Society and IOP Publishing Ltd

NTs by doping B/N pairs with an appropriate doping concentration, and the novel characteristics are potentially useful in future applications.

2. Method and model

For the investigation of the *ab initio* electronic band structure of MCNTs, we use the Vienna *ab initio* Simulation Package (VASP)[22] with its projected-augmented wave pseudopotentials.[23,24] The generalised gradient approximation (GGA)[25] and the Perdew–Wang 91 (PW91) exchange-correlation function are chosen. The energy cutoff for plane-wave basis is 400 eV and MCNTs are separated from each other by 10 Å (1 Å=0.1 nm) of vacuum in our calculation. A Monkhorst–Pack k grid of $1 \times 1 \times 11$ is used for the one-dimensional (1D) Brillouin zone (BZ). All atoms in the unit cell are allowed to relax, and the force tolerance is set at 0.01 eV/Å. We choose a $1 \times 1 \times 21$ Line-mode k-point grid to calculate the energy band. For the density of states (DOS) calculation, we use the tetrahedron integration method with a $1 \times 1 \times 21$ k grid.

Using the thermodynamic approach, we have a comparative analysis of energy stability of the structures shown in Fig. 1. The formation energy[26] $E_{\rm f}$ of doped CNTs is calculated from the following equation:

$$E_{\rm f} = (E_{\rm t1} - E_{\rm t2}) - m(E_1 - E_2), \tag{1}$$

where $E_{\rm t1}$ is the total energy of CNTs with substitutional doping, $E_{\rm t2}$ is the total energy of pristine CNTs, E_1 is the energy of single free doping atom, E_2 is the energy of single free carton atom, and m is the number of doping atoms.

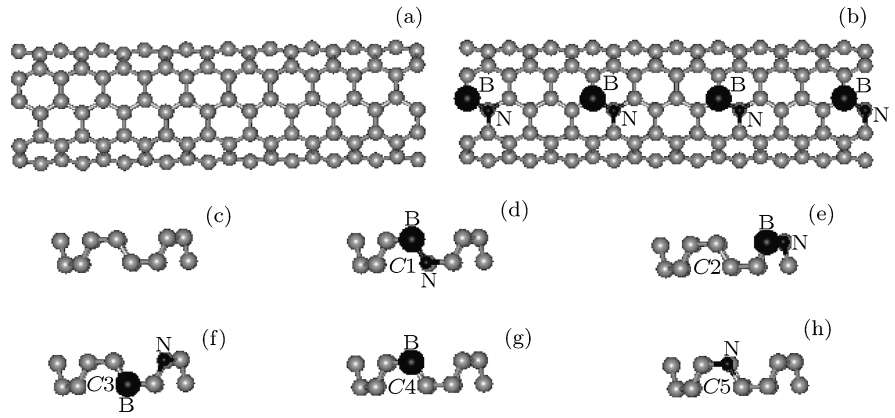


Fig. 1. Schematic view of armchair (5,5) MCNTs, showing (a) pristine MCNTs, (b) doped MCNTs, and (c)–(h) unit cells of doped MCNTs. The grey, large black, and small black balls correspond to carbon, boron, and nitrogen atoms, respectively.

We also perform first-principles transport calculation based on the pseudopotential density-functional theory and investigate the electronic transport properties of MCNTs modulated with different doping configurations shown in Fig. 2. The transport properties of MCNTs are calculated based on nonequilibrium Green's function formalism as implemented in ATK (Atomistix ToolKit),[27] which is based on real-space, nonequilibrium Green's function (NEGF) formalism and the density-functional theory (DFT). The approximation for the exchange-correlation functional is the spin-unpolarised generalised gradient approximation (GGA). The conductance can be calculated by the Landauer–Büttiker formula[28,29] in which the entire system is divided into three parts: the central region and two leads. The calculation for electrode part is performed under periodical boundary conditions, with the unit cell being four atomic layers along the tube axis and the k-point grid being $1 \times 1 \times 50$. Self-consistent calculations are performed with a mixing rate set to be 0.02, and the mesh cutoff of carbon atom is 120 Ry to achieve a balance between calculation efficiency and accuracy. The C–C bond length is chosen to be 1.425 Å before geometry optimisation, and these parameters were tested in the previous work.

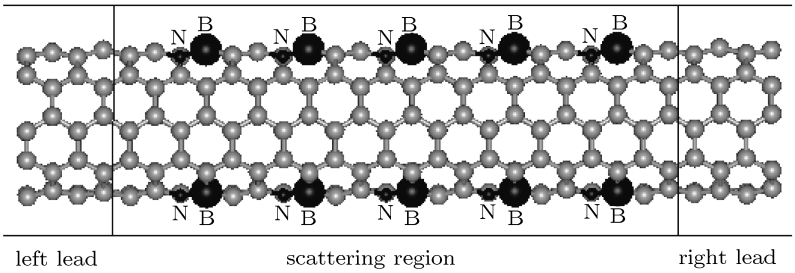


Fig. 2. Structures of the extended armchair (5,5) MCNTs junction, showing that an MCNT junction is coupled to two semi-infinite MCNT electrodes, and the 220 (eleven unit cells for tubes) atoms for different doping armchair (5,5) MCNTs are in the device scattering region.

The conductance is given in the Landauer–Büttiker formalism as

$$\boldsymbol{G}(\boldsymbol{E}) = \boldsymbol{G}_0 \,\mathrm{Tr}[\Gamma_{\mathrm{L}}(\boldsymbol{E})\boldsymbol{G}^{r}(\boldsymbol{E})\Gamma_{\mathrm{R}}(\boldsymbol{E})\boldsymbol{G}^{\mathrm{a}}(\boldsymbol{E})], \quad (2)$$

where $\boldsymbol{G}_0 = 2e^2/h$ is the conductance quantum, $\boldsymbol{G}^{\mathrm{r(a)}}(\boldsymbol{E}) = [\boldsymbol{E}\cdot\boldsymbol{I} - \boldsymbol{H} - \Sigma_{\mathrm{L}}^{\mathrm{r(a)}} - \Sigma_{\mathrm{R}}^{\mathrm{r(a)}}]^{-1}$ is the retarded (advanced) Green's function matrix of the central part, $\Sigma_{\mathrm{L(R)}}^{\mathrm{r(a)}}(\boldsymbol{E})$ is the retarded (advanced) self-energy due to the left and the right electrodes, and $\Gamma_{\mathrm{L(R)}}(\boldsymbol{E}) = \mathrm{i}[\Sigma_{\mathrm{L(R)}}^{r}(\boldsymbol{E}) - \Sigma_{\mathrm{L(R)}}^{\mathrm{a}}(\boldsymbol{E})]$ is the contact broadening functions associated with the left (right) electrodes, with $\boldsymbol{I}$ being the unitary matrix and $\boldsymbol{H}$ being the corresponding matrix element Hamiltonian.

3. Results and discussion

We investigate the effect of B/N pair co-doping on the energy structure and the transport properties of armchair MCNTs. Here we study MCNTs with a set of different concentrations of B/N pairs, elucidating (i) the role of the doping sites of the B/N pairs; (ii) the effect of doping concentration on electronic structure both around the tube and along the tube axis; (iii) transport properties at different doping concentrations. Firstly, we substitute one pair of adjacent C atoms of MCNT with one B atom and one N atom in the unit cell of MCNTs as shown in Fig. 1. For armchair (5,5) MCNT, we calculate the formation energies of five possible configurations shown in Figs. 1(d)–1(h). The formation energies of armchair (5,5) MCNT are given in Table 1. The formation energy of $C1$ configuration shown in Fig. 1(d) is 1.910 eV, which means that $C1$ configuration is a most stable structure. The formation energy results show that B/N pairs are easier to dope into MCNTs than either B or N alone.

Table 1. Formation energies of different configurations of doped armchair (5,5) MCNTs.

configuration	E_{f}/eV
$C1$	1.910
$C2$	2.825
$C3$	4.631
$C4$	3.532
$C5$	1.968

For energy band calculations, we consider the sensitivity of electronic structure property to doping concentration. Three unit cell models of armchair (5,5) MCNTs with different circumferential concentrations are indicated in Fig. 3(a). Figure 3(b) presents the total DOS as a function of energy scaled by Fermi energy for pristine tube, doping tubes of $d = 5\%$ and 10%, where d represents circumferential concentration of B/N pair co-doping, i.e. the ratio of the number of doping atoms to that of total atoms in the unit cell of MCNTs. From the DOS curves, we find that the width of zero gap near the Fermi level increases with the increase of circumferential concentration. We find that the energy gap values for the cases of $d = 5\%$, and 10% increase from 0.222 to 0.432 eV in Fig. 3(c). We also find that pristine armchair (5,5) MCNTs have no energy gap at the Fermi level and the energy gap increases with the increase of circumferential concentration in doped MCNTs. It means that the energy gap strongly depends on doping concentration. These results accord well with those presented by Xu *et al.*,[18] which suggests that the energy gap depends on doping concentration

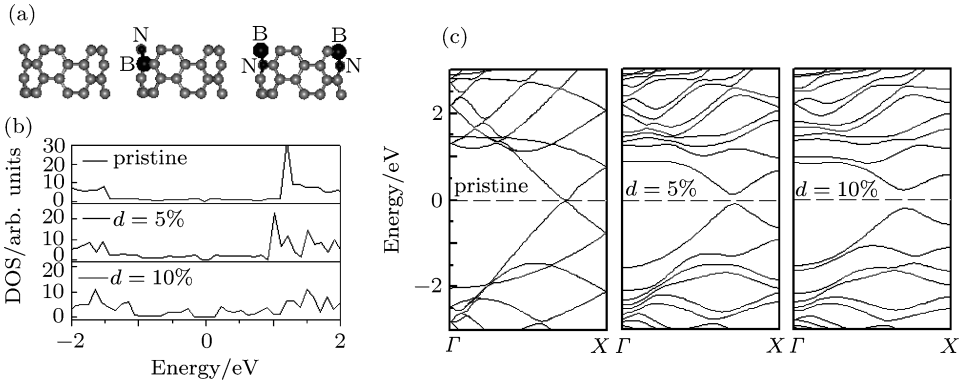


Fig. 3. (a) Three unit cell models of armchair (5,5) MCNTs with different circumferential concentrations, (b) the densities of states, and (c) band structures each as a function of energy scaled by Fermi energy for pristine tubes, at two values of d, i.e. $d = 5\%$ and 10%, where d represents circumferential concentration of B/N pairs doped. The Fermi level is indicated with black dash line.

We also study the electronic structure properties of armchair MCNTs with different axial concentrations of B/N pairs. Figure 4(a) shows three unit cell models of armchair (5,5) MCNTs with different axial concentrations. We present the total DOS as a function of energy shown in Fig. 4(b), scaled by Fermi energy for $L = 0.407$, $L = 0.203$, and $L = 0.102$ Å^{-1}, where L represents axial concentrations of B/N pairs doped, which is the reciprocal of the unit cell axial size in MCNTs. The total DOS curves reveal that the width of zero gap near the Fermi level decreases with the reduction of axial concentration. Figure 4(c) shows the band gaps for $L = 0.407$, 0.203, and 0.102 Å^{-1} are 0.246, 0.206, and 0.13 eV respectively. The model with $d = 5\%$ in Fig. 3(a) and the model with $L = 0.203$ Å^{-1} in Fig. 4(a) have the same B/N pair doping concentrations. At the same concentration of B/N pairs, the positions of B/N pairs doped in MCNTs are different. The difference in B/N pair position leads to differences in DOS curve and in energy gap. It is shown that the energy gap strongly depends on doping concentration and decreases with doping concentration decreasing.

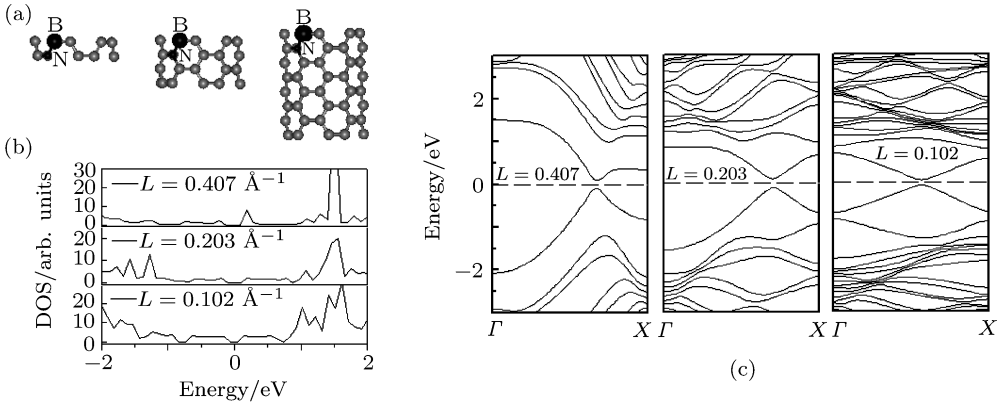


Fig. 4. (a) Three unit cell models of armchair (5,5) MCNTs with axial concentrations, (b) densities of states, and (c) band structures each as a function of energy scaled by Fermi energy for $L = 0.407$, $L = 0.203$, and 0.102 Å^{-1}, where L represents axial concentrations of B/N pairs doped. The Fermi level is indicated with black dash line.

To further explain the energy gap, we calculate the conductance of doped MCNTs contacted with metallic electrodes. As zero-bias conductance and transmission spectrum are related by a simple multiplicative factor, we plot the equilibrium transmission spectrum of doped MCNTs. We turn to the wave functions of the π (bonding states) and π^* (antibonding states) subbands, which are the only bands near the Fermi level and responsible for the electron transmission. Figure 5 shows the transmission spectra with different circumferential concentrations. Armchair MCNTs have two linear electronic energy bands which cross at the Fermi level and contribute two conductance quanta ($2G_0$) shown in Fig. 5(a). Figures 5(b) and 5(c) show transmission spectra with circumferential concentrations of B/N pairs: 5% and 10%, respectively. By comparison with the

transmission spectrum of the pristine MCTNs, these explicit changes shown in Figs. 5(b) and 5(c) include (i) the quantum step feature disappears; (ii) the conductance drops for most Fermi energies; (iii) associated with a zero gap of DOS, zero-conductance dip appears near the Fermi level; (iv) the width of zero-conductance dip near Fermi energy increases with doping concentration increasing. This critical value at which zero-conductance dip is obtained also depends on axial concentration of the MCNTs.

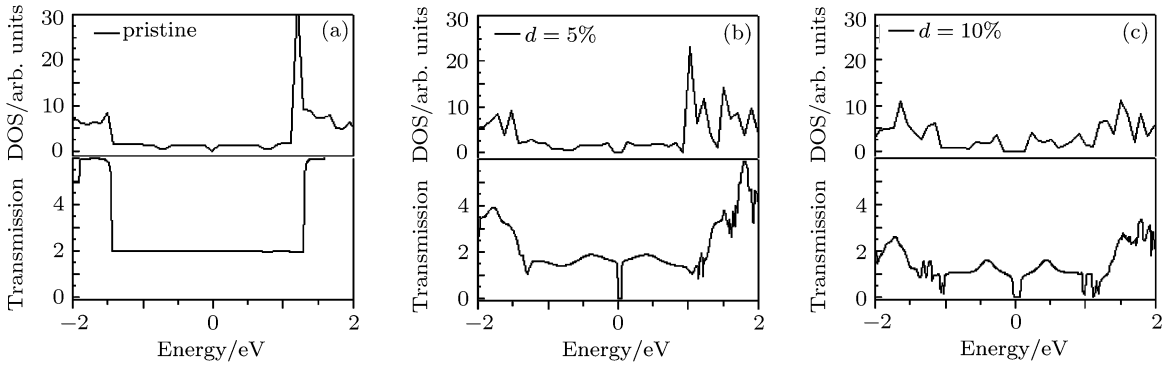


Fig. 5. Densities of states and transmission spectra each as a function of energy for armchair (5,5) MCNTs. (a) Pristine tubes, (b) $d = 5\%$, and (c) $d = 10\%$, where d represents circumferential concentration of B/N pairs doped.

Figure 6(a) preserves the quantum step feature for doping concentration ($L = 0.407$ Å^{-1}). The conductance shows one narrow dip and two broad dips, and the reduction of conductance at the broad dip is $1G_0$ with an approximately half the reflection of both π and π^* subbands for B/N pair impurities. Figures 6(b) and 6(c) show the transmission spectra with two axial concentrations for $L = 0.203$ and 0.102 Å^{-1}, respectively. We find that states near the Fermi level are strongly affected by the B/N pair impurities, yielding a full suppression of conductance near Fermi energy. In this case, the zero-conductance dip appears due to almost complete reflection of π and π^* subbands. The π and π^* bands are not mixed and the eigenchannels are completely reflected via resonant backscattering. The conductance dip also implies the appearing of energy gap, and consequently a transformation from metal to semiconductor happens.

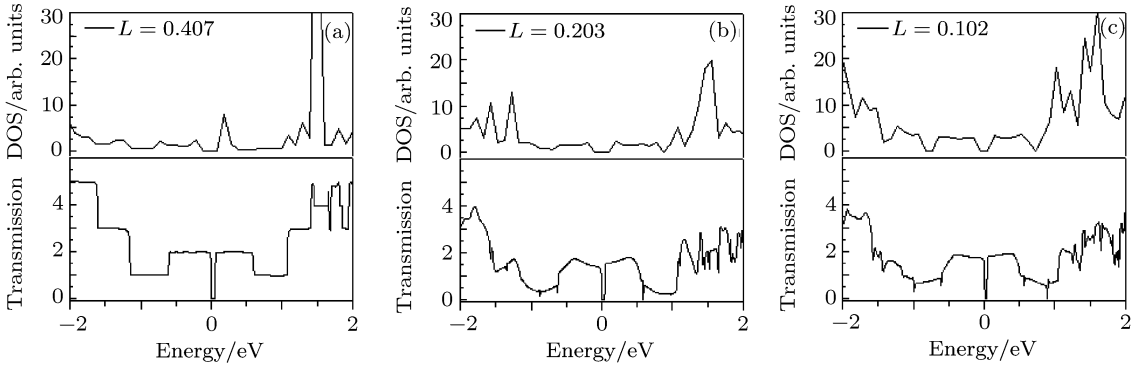


Fig. 6. The DOS and transmission spectra each as a function of energy for armchair (5,5) MCNTs. (a) $L = 0.407$ Å^{-1}, (b) $L = 0.203$ Å^{-1}, and (c) $L = 0.102$ Å^{-1}, where L represents axial concentration of B/N pairs doped.

With the energy band theory and the mirror symmetry breaking, this phenomenon will be explained. For either B or N doping alone in armchair MCNTs, substitutional doping with either boron or nitrogen atom produces quasibound impurity states. The band structures of only B doping and only N doping in armchair (5,5) MCNTs are shown in Figs. 7(a) and 7(b), respectively. It is interesting to notice that doping with B atom (p-type) reduces the number of the valence electrons and the Fermi level moves down through the valence band, while doping with N atom (n-type) enhances the number of the valence electrons

and the Fermi level moves up through the conduction band. Besides, a pristine tube has the mirror planes: one plane is perpendicular to the tube axis and the other plane is parallel to it, while the substitution of B or N atom preserves only one mirror plane containing the B or N atom and perpendicular to the tube axis. Because the mirror symmetry plane containing the tube axis is broken by either B or N impurity, there is a mixture of the π subband and the π^* subband at the Fermi level. Thus, doping with either B or N atom alone of CNTs tends to produce metallic behaviour. However, B/N pair co-doping does not increase the number of the valence electrons but introduce the quasibound impurity level, therefore there is almost no shift of the Fermi level after doping. Figure 7(c) shows the projected density of states (PDOS) of armchair (5,5) MCNTs with 5% circumferential concentration, which provides detailed information about electronic band structure corresponding to this configuration. We find that above the Fermi level the peaks of PDOS, created by an N atom, are higher than those by B and C atoms, and below the Fermi level the peaks of PDOS, created by an B atom, are higher than those by N and C atoms, which indicates that the bottom of conduction band is mainly contributed by the p-orbitals of substitutional N atoms and the top of valence band is contributed by the p-orbitals of substitutional B atoms. Our results also reveal that the bottom of conduction band moves up and the top of valence band moves down, and the amount of shift increases with the increase of doping concentration. B/N pair impurities break mirror symmetry planes perpendicular to the tube axis. The π subband and the π^* subband shift below and above the Fermi level, and B/N pair impurities cause the conductance to drop to zero via resonant backscattering. Therefore an energy gap generates triggering a metal-semiconductor transition.

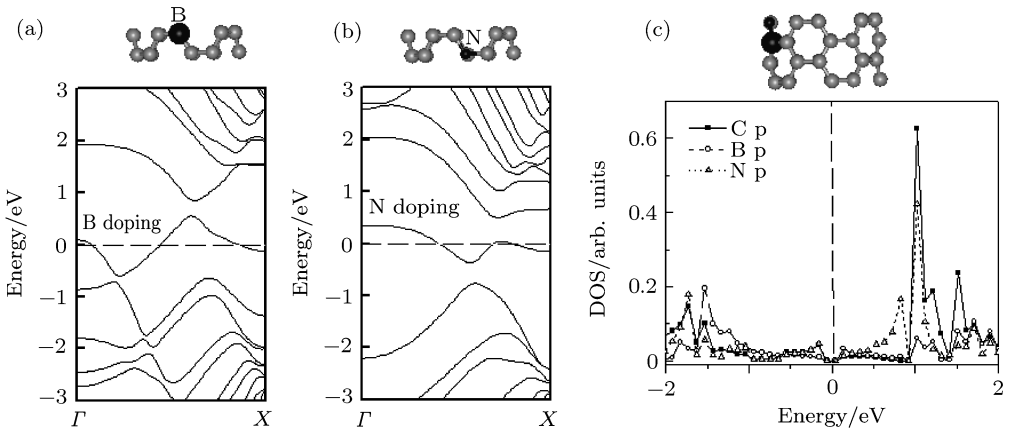


Fig. 7. (a) Unit cell model of armchair (5,5) MCNTs with B atom doping alone and its band structure as a function of energy, (b) unit cell model of armchair (5,5) MCNTs with N atom doping alone and its band structure as a function of energy, and (c) unit cell model of armchair (5,5) MCNTs with B/N pair co-doping and its PDOS in p-orbitals.

4. Conclusions

The *ab initio* calculations of electronic band structure and quantum transport properties of B/N pair co-doping armchair (5,5) MCNTs are reported. According to the formation energy of armchair MCNTs, B/N pair co-doping is the stablest structure and it is easy to co-dope into MCNTs lattices. Our results show that the energy gap of MCNTs strongly depends on the concentration of doped B/N pairs. The energy gap increases with the increase of doping concentration both around the tube and along the tube axis. As previously reported,[30] in the conductance results the energy spectrum features the pronounced dips at the corresponding energies. We find that the width of zero-conductance dip near Fermi energy increases with doping concentration increasing. We confirm that the physical origin of the phenomenon would be the mirror symmetry breaking of MCNTs, which triggers a metal-semiconductor transition in some extent to generate an energy gap. The novel characteristics are potentially useful for fabricating devices based on CNTs, such as semiconducting molecular wires, spintronic devices, field-effect transistors and field emission source.

References

[1] Iijima S 1991 *Nature* **354** 56

[2] Ni M Y, Wang X L and Zeng Z 2009 *Chin. Phys.* B **18** 357

[3] LeMieux M C, Roberts M, Barman S, Jin Y W, Kim J M and Bao Z 2008 *Science* **321** 101

[4] Mei L W, Zhang Z H and Ding K H 2009 *Acta Phys. Sin.* **58** 1971 (in Chinese)

[5] Liu X Y, Wang C Y, Tang Y J, Sun W G, Wu W D, Zhang H Q, Liu M, Yuan L and Xu J J 2009 *Acta Phys. Sin.* **58** 1126 (in Chinese)

[6] Chen G D, Wang L D, An B, Yang M, Cao D C and Liu G Q 2009 *Acta Phys. Sin.* **58** 1190 (in Chinese)

[7] Javey A, Guo J, Wang Q, Lundstrom M and Dai H G 2003 *Nature* **424** 654

[8] Park J Y 2007 *Nanotechnology* **18** 095202

[9] Qiao L, Wang C, Qu C Q, Zeng Y, Yu S S, Hu X Y, Zheng W T and Jiang Q 2009 *Diam. Relat. Mater.* **18** 657

[10] Chopra S, McGuire K, Gothard N, Rao A M and Pham A 2003 *Appl. Phys. Lett.* **83** 2280

[11] Lee K W, Heo K Y, Kim K M and Kim H J 2009 *Nanotechnology* **20** 6

[12] Lee K W, Heo K Y and Kim H J 2009 *Appl. Phys. Lett.* **94** 102112

[13] Lu B and Zhou Z 2007 *Carbon* **45** 2105

[14] Murata N, Haruyama J, Reppert J, Rao A M, Koretsune T, Saito S, Matsudaira M and Yagi Y 2008 *Phys. Rev. Lett.* **101** 027002

[15] Shlyakhova E V, Yudanov N F, Shubin Yu V, Yudanova L I, Bulusheva L G and Okotrub A V 2009 *Carbon* **47** 1701

[16] Hsu W K, Chu S Y, Munoz-Picone E, Boldu J L, Firth S, Franchi P, Roberts B P, Schilder A, Terrones H, Grobert N, Zhu Y Q, Terrones M, McHenry M E, Kroto H W and Walton D R M 2000 *Chem. Phys. Lett.* **323** 572

[17] Terrones M, Ajayan M, Banhart F, Blase X, Carroll D L, Charlier J C, Czerw R, Foley B, Grobert N, Kamalakaran R, Redlich P K, Rühle M, Seeger T and Terrones H 2002 *Appl. Phys.* A **74** 355

[18] Xu Z, Lu W G, Wang W L, Gu C Z, Liu K H, Bai X D, Wang E G and Dai H J 2008 *Adv. Mater.* **20** 3615

[19] Wang W L, Bai X D, Liu K H, Xu Z, Golberg D, Bando Y and Wang E G 2006 *J. Am. Chem. Soc.* **128** 6530

[20] Stephan O, Ajayan P M, Colliex C, Redlich P, Lambert J M, Bernier P and Lefin P 1994 *Science* **266** 1683

[21] Buonocore F 2007 *Philosophical Magazine* **87** 1097

[22] Li Y T and Chen T C 2009 *Nanotechnology* **20** 375705

[23] Blöchl P E, Forst C and Schimpl J 2003 *Bull. Mater. Sci.* **26** 33

[24] Blöchl P E 1994 *Phys. Rev.* B **50** 17953

[25] John P P, Kieron B and Matthias E 1996 *Phys. Rev. Lett.* **77** 3865

[26] Yu S S, Zheng W T, Wen Q B and Jiang Q 2008 *Carbon* **46** 537

[27] Ouyang F P, Xiao J, Guo R, Zhang H and Xu H 2009 *Nanotechnology* **20** 055202

[28] Sahin H and Senger R T 2008 *Phys. Rev.* B **78** 205423

[29] Yan J Y, Zhang P, Sun B, Lu H Z, Wang Z G, Duan S Q and Zhao X G 2009 *Phys. Rev.* B **79** 115403

[30] Hyoung J C, Jisoon I, Steven G L and Marvin L C 2000 *Phys. Rev. Lett.* **84** 13